Journal of Experimental Botany
https://doi.org/10.1093/jxb/erad113 Advance Access Publication 25 March, 2023

RESEARCH PAPER

Combining quantitative trait locus mapping with multiomics profiling reveals genetic control of corn leaf aphid (*Rhopalosiphum maidis*) resistance in maize

Tengyue Wang[1,†], Kaiji Wang[1,†], Chuanhong Wang[1], Yibing Zhao[1], Zhen Tao[1], Junyao Li[1], Lei Wang[1], Jian Shi[1], Shijie Huang[1], Chuanxiao Xie[2,*] and Peijin Li[1,*]

[1] National Key Engineering Lab of Crop Stress Resistance Breeding, School of Life Sciences, Anhui Agricultural University, Hefei, 230036, China
[2] Institute of Crop Science, Chinese Academy of Agricultural Sciences, No. 12 Zhongguancun South Street, Haidian District, Beijing, 100081, China

[†] These authors contributed equally to this work.
* Correspondence: xiechuanxiao@caas.cn or peijin.li@ahau.edu.cn

Received 26 September 2022; Editorial decision 21 March 2023; Accepted 22 March 2023

Editor: Robert Hancock, The James Hutton Institute, UK

Abstract

The corn leaf aphid (*Rhopalosiphum maidis*) is a major maize pest that frequently causes substantial yield losses. Exploring the genetic basis of resistance to aphids is important for improving maize yield and quality. Here, we used a maize recombinant inbred line population derived from two parents with different susceptibility to aphids, B73 (susceptible) and Abe2 (resistant), and performed quantitative trait locus (QTL) mapping using aphid resistance scores as an indicator. We mapped a stable QTL, *qRTA6*, to chromosome 6 using data from 2 years of field trials, which explained 40.12–55.17% of the phenotypic variation. To further investigate the mechanism of aphid resistance in Abe2, we constructed transcriptome and metabolome libraries from Abe2 and B73 leaves with or without aphid infestation at different time points. Integrating QTL mapping and transcriptome data revealed three aphid resistance candidate genes (Zm00001d035736, Zm00001d035751, and Zm00001d035767) associated with the hypersensitive response, the jasmonic acid pathway, and protein ubiquitination. Integrated transcriptomic and metabolomic analysis revealed that the differentially expressed genes and metabolites were enriched in flavonoid biosynthesis. These findings extend our understanding of the molecular mechanisms controlling aphid resistance in maize, and the QTL and candidate genes are valuable resources for increasing this resistance.

Keywords: Aphid resistance, flavonoids, maize, metabolome, QTL mapping, transcriptome.

Abbreviations: BX, benzoxazinoid; DAM, differentially accumulated metabolite; DEG, differentially expressed gene; ET, ethylene; FPKM, fragments per kilobase of exon per million reads mapped; FDR, false discovery rate; JA, jasmonic acid; KEGG, Kyoto Encyclopedia of Genes and Genomes; RT–qPCR, reverse transcription–quantitative PCR; QTL, quantitative trait locus; RIL, recombinant inbred line; RNA-seq, RNA sequencing; SA, salicylic acid; SLAF, specific-locus amplified fragment sequencing; VIP, variable importance on projection.

Introduction

Maize (*Zea mays* L., 2*n*=20) is a staple food crop for many regions throughout the world and an important raw material for forage, industry, and biofuels; thus, improving maize quality and yield is critical to ensure global food security. However, maize experiences a variety of environmental and biological stresses throughout its growing period, including insect pests (Meihls *et al.*, 2012). Global climate change, changes in farming systems, and monocropping have made pest outbreaks more frequent, seriously threatening maize productivity.

The corn leaf aphid (*Rhopalosiphum maidis*) is a destructive pest that feeds on the sap of maize plants, resulting in stunted growth and sometimes plant death (Zogli *et al.*, 2020). In the vegetative stages of maize growth, aphids feed on leaves and secrete honeydew, which supports the growth of black mold that severely limits the plant's photosynthetic efficiency. At the reproductive stages, aphids infest the tassels, hindering pollen development and reducing yield (Carena and Glogoza, 2004). Aphids also act as vectors for plant viruses such as maize dwarf mosaic virus, which causes serious disease in field crops (Brault *et al.*, 2010). Farmers primarily use chemical insecticides to control aphid populations, but excessive pesticide application selects for the evolution of insecticide resistance and harms natural ecosystems. Therefore, screening for aphid-resistant materials from natural maize genetic resources and breeding aphid-resistant maize lines is a more sustainable and cost-effective approach to control aphids and protect maize yield potential.

Plants and insects have co-evolved in an 'arms race' during which plants evolved various direct and indirect defenses against pest attack (Qi *et al.*, 2018). Chemical defense mechanisms include the production of secondary metabolites and other components that are not conducive to digestion by insects. The secondary metabolites mainly include phenolics, terpenoids, and nitrogenous compounds. Benzoxazinoids (BXs) are important secondary metabolites in maize that suppress phytophagous pests by releasing toxic glycosidic ligands (Ahmad *et al.*, 2011; Handrick *et al.*, 2016). When attacked by insects, some plants release a series of volatile secondary compounds (Loreto and D'Auria, 2021) such as (3*E*)-4,8-dimethyl-1,3,7-nonatriene (Chen et al., 2021, 2022), (*E*,*E*)-4,8,12-trimethyl-1,3,7,11-tridecatetraene (Richter *et al.*, 2016), and (*E*)-β-farnesene (Wang *et al.*, 2022a). These compounds enhance the attraction of natural enemies, inhibit insect feeding and egg laying, and act as signals to neighboring plants to ward off the insect threat, a process referred to as indirect defense. Phytohormones also play important roles in plant defense responses (Erb and Reymond, 2019). Phytohormone interactions form a complex regulatory network, in which the jasmonic acid (JA) and salicylic acid (SA) pathways act as the main signaling pathways in plant defense (Berens *et al.*, 2016; Costarelli *et al.*, 2019). Ethylene (ET) signaling pathways are also involved in resistance to insects (Louis *et al.*, 2015; Ma *et al.*, 2020). Plant signaling pathways including JA, SA, ET, abscisic acid, and gibberellic acid induce changes in the expression of defense genes, which lead to metabolic changes enhancing plant defenses in response to aphid attack (Morkunas *et al.*, 2011). Abscisic acid and JA play important roles in constitutive defense in the tolerance of soybean genotype KS4202 to the soybean aphid (Chapman *et al.*, 2018). In Arabidopsis, AtWRKY22 was reported to promote susceptibility to aphids by modulating the interplay between the SA and JA signaling (Kloth *et al.*, 2016).

The availability of maize genome sequences, such as that of the line B73, has facilitated dissection of the genetic basis of aphid resistance (Schnable *et al.*, 2009). Resistance to aphids is a quantitative trait controlled by multiple small-effect quantitative trait loci (QTLs), and several QTLs associated with aphid resistance in maize have been identified. Meihls *et al.* (2013) used a recombinant inbred line (RIL) population generated from B73 and CML322 to map aphid-resistance loci using the contents of 2,4-dihydroxy-7-methoxy-l,4-benzoxazin-3-one (DIMBOA) and 2-hydroxy-4,7-dimethoxy-1,4-benzoxazol-3-one (HDIMBOA) as indicators, and found three homologs of the BX biosynthesis gene *BX7* at the bin1.04 region (Meihls *et al.*, 2013). Betsiashvili *et al.* (2015) used the aphid-susceptible line B73 and the aphid-resistant line Mo17 to construct a RIL population to study aphid resistance using aphid reproduction number and DIMBOA content as indicators, and identified two major QTLs on chromosomes 4 and 6. Furthermore, Tzin *et al.* (2015b) used a RIL population generated from a cross of B73 and Ky21 and located aphid-resistance loci on chromosomes 1, 7, and 10 using aphid reproduction rate as an indicator. However, the molecular mechanisms responsible for aphid resistance are still poorly understood. Therefore, it is critical to explore new aphid-resistance genes and their underlying mechanisms.

The rapid development of omics technologies (e.g. transcriptomics, metabolomics, and proteomics) has facilitated the study of genes involved in defense responses to aphids (Yu *et al.*, 2015). Tzin *et al.* (2015a) analyzed the transcriptome and metabolome of maize leaves from 2 h to 96 h after aphid infestation and found that BX and volatile terpene biosynthesis are involved in aphid defenses. Transcriptomic and metabolomic analysis of lines B73 and Mo17 identified four transcription factors (TFs), MYB (GRMZM2G108959), GRAS (GRMZM2G015080), NAC (GRMZM2G179049), and WRKY (GRMZM2G425430), that might be responsible for the high accumulation of BXs in Mo17 and consequently this line's resistance to aphids (Song *et al.*, 2017). Pingault *et al.* (2021) analyzed the aphid defense responses of the resistant inbred line Mp708 and the susceptible inbred line Tx601 at the transcriptome and volatile metabolite levels, and proposed that the activation of phytohormone pathways, the inducible expression of sesquiterpene synthase and terpene synthase genes, and the biosynthesis of volatile organic compounds play

important roles in the direct or indirect defense responses in maize. Bai *et al.* (2022) used a combination of forward and reverse genetics, transcriptomics, untargeted metabolomics, and nuclear magnetic resonance to identify a plant-specific metabolite, CP-5-(*Z*)-3-hexenal, involved in non-host resistance to leafhoppers. However, the combination of QTL mapping and multiomics analysis to identify candidate genes for aphid resistance has not been reported in maize.

Here, we performed QTL mapping in a maize RIL population and identified a stable QTL for resistance to aphids. Following infestation of the maize plants by *R. maidis*, we analyzed transcriptomic and metabolic changes in the leaves of the susceptible line B73 and the resistant line Abe2 to identify candidate genes, metabolites, and key pathways. We aimed to (i) study the genetics of aphid resistance using a QTL mapping approach, (ii) compare the transcriptomic and metabolic profiles of B73 and Abe2 in the absence and presence of aphid infestation, and (iii) identify candidate resistance genes by combining QTL mapping and transcriptome data. Our findings improve understanding of the molecular mechanism underlying aphid resistance and provide candidate resistance genes for breeding aphid-resistant maize.

Materials and methods

Aphid bioassays

The corn leaf aphid *R. maidis* was cultured on seedlings of the susceptible maize line B73. To evaluate *R. maidis* fecundity, 20 apterous adults were transferred to the middle of the third leaves. After 14 d, the total number of aphids on each maize plant was counted. Twelve aphid-inoculated maize plants were used as replicates for each assay. To evaluate the period from birth to the first reproduction, one new neonate was placed on the middle of the third leaf of each plant and the aphid propagation profile was recorded until its first reproduction. Each group included 20 individual maize plants as replicates (Kettles *et al.*, 2013).

To test the aphids' preference for the maize lines, B73 and Abe2 plants were planted separately in the greenhouse and grown until the three-leaf stage. Pots containing individual B73 and Abe2 plants were placed next to each other and the two pots were connected by soil so that the aphids could move freely in and between both pots. Twenty aphids were placed in the middle position with equal distance to the two pots; after 24 h, the number of aphids on each seedling was counted and compared. Twelve replicates were set up for each experiment.

Plant materials and phenotype evaluation

The $F_{2:8}$ RIL population, consisting of 261 individuals, was developed using the single-seed descent method from the parental lines Abe2 and B73 (Liu *et al.*, 2016). These two lines show dramatically different resistance to aphids: Abe2 is resistant and B73 is susceptible. The parents and RILs were planted under natural growth conditions in the experimental base of Anhui Agricultural University in Sanya, Hainan Province, China (18°21′ N, 109°10′ E) in November of 2018 and 2020. A randomized complete-block design was used. Twenty plants of each line or parent were grown in two rows; the distance between two adjacent rows was 20 cm and the space between two individuals was 50 cm. Field management was consistent across the plots, without pesticide applications.

The number of aphids on each maize line was counted at the peak of the aphid season (heading stage). The aphid resistance levels of individual RILs and the parents were scored on a five-point rating scale according to the relative aphid coverage, as shown in Supplementary Fig. S1. Scoring was performed based on previous studies (Liang *et al.*, 2016; Zhang *et al.*, 2021).

QTL analysis

A high-density single-nucleotide polymorphism (SNP) genetic map of the $F_{2:8}$ RIL population was constructed by specific-locus amplified fragment (SLAF) sequencing (Zeng *et al.*, 2020; Shi *et al.*, 2022). The sequencing reads were aligned to the B73_v4 reference genome (Jiao *et al.*, 2017) using BWA software, and then the SLAF markers were identified and genotyped. A genetic map containing 10 114 SNPs with an average map distance of 0.16 cM between adjacent markers was used for QTL mapping.

QTL mapping was conducted by using the composite interval mapping method in R/qtl; the QTL threshold was determined by a permutation test ($P<0.05$) and the QTL region was determined. The additive effects and phenotypic contribution rates of QTLs were calculated from the QTL results. QTLs were named following the protocol of Mccouch *et al.* (1997). Using '*qRTA06-1*' as an example, '*q*' refers to QTL, '*RTA*' refers to resistance to aphids, '*06*' indicates the chromosome, and '*1*' indicates the number of the QTL. The 1 logarithm of the odds (1-LOD) and 2-LOD support intervals were determined per trait.

Transcriptome analysis

For RNA sequencing (RNA-seq), the susceptible B73 and resistant Abe2 lines were grown to the three-leaf stage in the greenhouse. Then, 15 adult aphids were gently placed on the middle of the second leaf. The plants of the control group were grown in parallel with the treatment groups but without aphid infestation. At least six leaves were collected from different plants for each sample at 0, 6, and 24 hours post infestation (hpi). Each treatment had three biological replicates. A total of 18 samples were collected (i.e. three biological replicates×three time points×two genotypes). Samples were immediately frozen in liquid nitrogen and stored at −80 °C until use.

Total RNA from all samples was isolated and purified using TRIzol reagent (Invitrogen). A NanoDrop ND-1000 (ThermoFisher) was used to control the amount and purity of RNA, and then a Bioanalyzer 2100 (Agilent) was used to measure RNA integrity. The cDNA libraries were sequenced with a read length of 150 bp (paired-end) using the Illumina Novaseq 6000 System at Lianchuan Biotechnology Company (Hangzhou, China). The raw RNA-seq read data were deposited in the NCBI Sequence Read Archive (https://www.ncbi.nlm.nih.gov/sra) under accession number PRJNA871985.

The sequencing data were filtered to obtain high-quality clean reads, which were compared to the reference maize genome B73_v4 (Jiao *et al.*, 2017). The fragments per kilobase of exon per million reads mapped (FPKM) value was used to normalize and estimate gene expression values (Trapnell *et al.*, 2012). Differential expression analysis was performed using the DESeq package (Love *et al.*, 2014). The resulting *P*-values were adjusted to control the false discovery rate (FDR). The parameters used to screen differentially expressed genes (DEGs) were $|\log_2(\text{fold change})| \geq 1$ and FDR<0.05 (Mu *et al.*, 2021). Differential expression was investigated in two ways: (i) for each genotype between the three time points (0, 6, and 24 hpi) and (ii) for each time point between the two genotypes. The R package 'clusterProfiler' was used for Kyoto Encyclopedia of Genes and Genomes (KEGG) enrichment analysis (Yu *et al.*, 2012). TBtools was used to construct the Venn diagram and heatmap (Chen *et al.*, 2018). TFs were identified with the PlantTFDB 4.0 database (http://planttfdb.cbi.pku.edu.cn) (Jin *et al.*, 2017).

Reverse transcription–quantitative PCR analysis

Total RNA was extracted from maize leaves with or without aphid infestation using TRIzol reagent (Invitrogen). First-strand cDNA was synthesized using the QuantiTect Reverse Transcription Kit (QIAGEN) following the manufacturer's instructions. Reverse transcription–quantitative PCR (RT–qPCR) was performed using SYBR Green mix (Quanti Nova SYBR Green PCR Kit, Roche). The genes encoding glyceraldehyde 3-phosphate dehydrogenase (*GADPH*) and *Ubiquitin* served as internal controls for normalizing gene expression, and the relative gene expression data were calculated by the $2^{-\Delta Ct}$ method. Gene expression analysis was carried out with three biological replicates and three technical replicates. The primer sequences for each gene are listed in Supplementary Table S1.

Metabolomic analyses

For the metabolomic analyses, maize plants were grown at the same time as the plants used for transcriptome sequencing analysis. Leaves of B73 and Abe2 at 24 hpi were used for untargeted metabolomics analysis, with uninfested leaves as controls. Each sample had five independent biological replicates, and each replicate included a pool of six leaves. Metabolomic analysis was conducted by Shanghai Bioprofile Technology Co., Ltd (Shanghai, China).

Metabolites were extracted using 1 ml of a precooled mixture of methanol, acetonitrile, and water (v/v/v, 2:2:1) and then subjected to 1 h ultrasonic shaking in an ice bath. Subsequently, the mixture was kept at –20 °C for 1 h and then centrifuged at 14 000 *g* for 20 min at 4 °C. The supernatants were recovered and concentrated to dryness in a vacuum. Metabolomics profiling was conducted using a UPLC-ESI-Q-Orbitrap-MS system (UHPLC, Shimadzu Nexera X2 LC-30AD, Shimadzu, Japan) coupled with Q-Exactive Plus (Thermo Scientific). The raw mass spectrometry data were processed using MS-DIAL for peak alignment, retention time correction, and peak area extraction. The metabolites were identified by accuracy mass (mass tolerance<0.01 Da) and tandem mass spectrometry data (mass tolerance<0.02 Da), which were matched with the Human Metabolome Database, MassBank, and other public databases, and a self-built metabolite standard library. In the extracted-ion features, only the variables having >50% of the non-zero measurement values in at least one group were kept.

The variable importance on projection (VIP) value indicates the contribution of a variable to the discrimination between all classes of samples. Metabolites with $P \leq 0.05$, VIP>1.0, or fold change ≥2 and $P \leq 0.5$ were considered to be statistically significant metabolites (Wang *et al.*, 2022b). Fold change was calculated as the logarithm of the average mass response (area) ratio between two samples.

The Pearson correlation coefficient of the DEGs and differentially accumulated metabolites (DAMs) was calculated using the cor function in R (version 4.0.1). The co-expression network was visualized using Cytoscape version 3.8.2 (Shannon *et al.*, 2003).

Results

Determining the aphid resistance of the parental lines B73 and Abe2

To screen for aphid-resistant and -susceptible maize germplasm as suitable parents for QTL mapping, we planted over 340 maize inbred lines in the field and allowed them to grow with no pesticides. Two years of field screening revealed that B73 was relatively susceptible to *R. maidis*, whereas Abe2 was resistant. To verify the field results, we tested B73 and Abe2 plants in the greenhouse. We observed many aphids on the tassels and lower leaves of B73, whereas these tissues were nearly free of aphids in Abe2 (Fig. 1A). Quantitative analysis of the aphid number revealed significant differences between the two inbred lines (Fig. 1B). When offered B73 and Abe2 leaves in a preference test, the aphids did not show a preference between them (Fig. 1C). To test aphid fecundity, we placed 20 adult aphids at the center of the third true leaf of three-leaf-stage plants and counted the number of aphids (including neonates) on each plant after 10 d. Abe2 seedlings had far fewer aphids than B73 seedlings (Fig. 1D). In addition, it took ~8 d for neonates to produce offspring on B73, but 10 d on Abe2 (Fig. 1E). These results indicate that B73 is relatively susceptible to *R. maidis*, whereas Abe2 is relatively resistant. Therefore, we chose B73 and Abe2 as the parents for our QTL mapping population.

Identifying genetic loci conferring aphid resistance by QTL mapping

We used the aphid resistance scores obtained from the field-grown RIL population in 2018 and 2020 and our genetic linkage map to conduct QTL mapping. We detected two significant QTLs (*qRTA6-1* and *qRTA6-2*) for aphid resistance on chromosome 6 across the 2 years (Fig. 2). These QTLs had a positive additive effect, suggesting that the allele carried by Abe2 acts to increase resistance to aphids. The QTLs also had overlapping confidence intervals, so we considered them to be the same QTL, named *qRTA6*. *qRTA6* explained 40.12% and 55.17% of the phenotypic variation in the 2 years, respectively (Table 1). We identified the physical location of *qRTA6* in the B73_V4 reference genome and found that *qRTA6* had a confidence interval of 0.78 Mb and contained 27 annotated genes (Supplementary Table S2).

Comparison of the transcriptome between Abe2 and B73

To study the effect of *R. maidis* infestation on maize gene expression, we collected the second true leaves from the resistant line Abe2 and the susceptible line B73 at 0, 6, and 24 hpi with 15 adult aphids. Each treatment had three biological replicates, resulting in a total of 18 samples being sent for transcriptome sequencing (RNA-seq). We obtained 0.80 billion raw reads from the 18 libraries, among which 0.72 billion clean reads were uniquely mapped to the B73_v4 reference genome, with a mapping rate ranging from 82.08% to 94.59% (Supplementary Table S3), suggesting that the genetic background of B73 and Abe2 may be relatively different; similar results are also seen in other sequencing reports (Wang *et al.*, 2021). The correlation coefficients between pairs of biological replicates under the same treatment were >0.95, indicating that the RNA-seq data were of satisfactory quality (Supplementary Fig. S2).

To identify the DEGs in response to aphid infestation, we compared the numbers of genes that were differentially

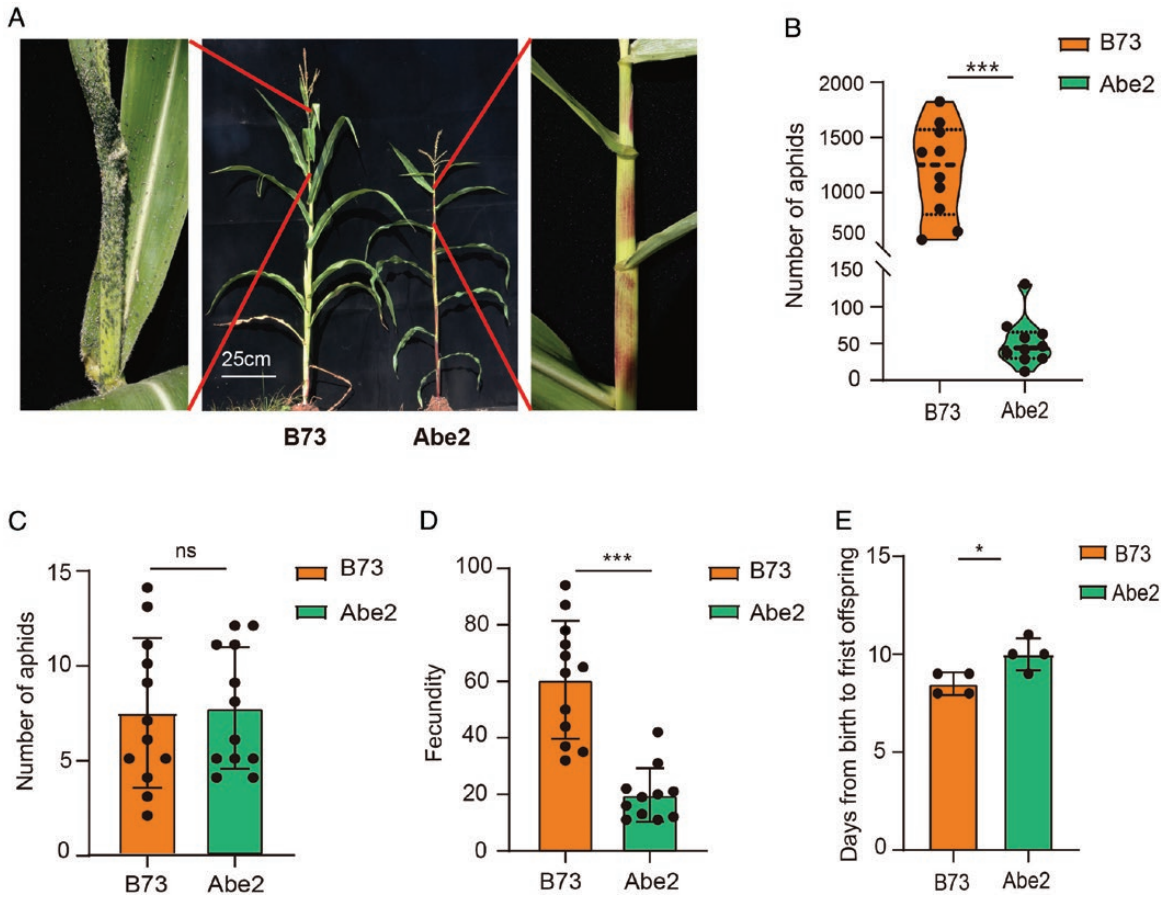

Fig. 1. Maize lines B73 and Abe2 show differential resistance to *R. maidis.* (A) Phenotype of B73 and Abe2 in the field upon aphid infestation. Scale bar=25 cm. (B) Quantitative comparison of aphid number on B73 and Abe2 (n=10). (C) Results of aphid preference tests comparing B73 and Abe2 (n=12). (D) Fecundity of aphids on B73 and Abe2 (n=12). (E) Number of days from birth to first offspring for aphids on B73 and Abe2 (n=4). Data are means ±SD; significant differences were determined using Student's t-test and are indicated with asterisks (*P<0.05, ***P<0.001; ns, not significant).

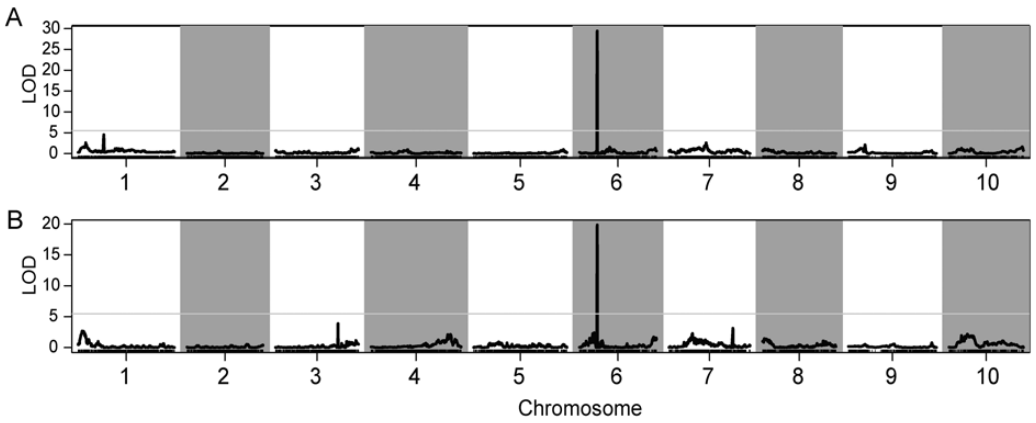

Fig. 2. QTLs detected for aphid resistance score in the B73×Abe2 RIL population in 2 years of field trials. (A) QTL mapping of aphid resistance score in 2018. (B) QTL mapping of aphid resistance score in 2020.

expressed between the control condition and the different infestation time points in B73 and Abe2 (Supplementary Table S4). For B73, we identified 3137 specific DEGs from B73 at 6 hpi (B73-6h) versus B73-0h, 2031 specific DEGs from B73-24h versus B73-0h, and 2722 specific DEGs from B73-24 h versus B73-6 h (Supplementary Fig. S3A). For Abe2, we detected 3405 specific DEGs from Abe2 at 6 hpi (Abe2-6h) versus Abe2-0h, 2988 specific DEGs from Abe2-24h versus

Table 1. QTLs detected for aphid resistance score in the B73×Abe2 RIL population

Trait	QTL name	Chromosome	QTL region (cM)	SLAF markers	Chromosome locations	LOD	Additive	R^2 (%)
2018RTA	*qRTA6-1*	6	34.94–35.72	Marker13386421–Marker14706484	43339216–46654245	29.42	0.352	55.17
2020RTA	*qRTA6-2*	6	34.94–35.72	Marker13386421–Marker14706484	43339216–46654245	19.85	0.823	40.12

Abe2-0h, and 3205 specific DEGs from Abe2-24h versus Abe2-6h (Supplementary Fig. S3B). Furthermore, we compared the number of DEGs in B73 and Abe2 at each time point. We identified 2890 specific DEGs from Abe2-0h versus B73-0h, 2549 specific DEGs from Abe2-6h versus B73-6h, and 2466 specific DEGs from Abe2-24h versus B73-24h, and 840 DEGs were common among all comparisons (Supplementary Fig. S3C). These results suggest that aphid infestation leads to dramatic transcriptional changes in maize.

To investigate the biological functions of the DEGs, we conducted KEGG pathway enrichment analysis of the DEG data. The DEGs between Abe2-0h and B73-0h were mainly involved in starch/sucrose metabolism, BX biosynthesis, glycine, serine, and threonine metabolism, monoterpenoid biosynthesis, terpenoid backbone biosynthesis, and glutathione metabolism (Supplementary Fig. S4A). At 6 hpi, the pathways were significantly enriched in starch/sucrose metabolism, glutathione metabolism, BX biosynthesis, monoterpenoid biosynthesis, and plant hormone signal transduction (Supplementary Fig. S4B). At 24 hpi, glutathione metabolism ranked as the top pathway enriched among the DEGs, followed by plant hormone signal transduction, starch/sucrose metabolism, terpenoid backbone biosynthesis, BX biosynthesis, monoterpenoid biosynthesis, and MAPK signaling pathway–plant (Supplementary Fig. S4C). Of these significantly enriched pathways, starch/sucrose metabolism, BX biosynthesis, monoterpenoid biosynthesis, and glutathione metabolism were enriched at all post-infestation time points. Plant hormone signal transduction and the MAPK signaling pathway may also play an important role in the response to aphid attack. Taken together, these results suggest that maize evolved numerous molecular defense strategies to respond to aphid infestation.

Plant hormone-related genes induced by aphid infestation

The phytohormones JA, SA, and ET play essential roles in orchestrating plant resistance against insects. KEGG enrichment analysis suggested that the phytohormone signaling pathways of maize are differentially regulated after aphid infestation. Therefore, we analyzed the expression of JA, SA, and ET biosynthesis genes in B73 and Abe2.

JA biosynthesis starts with α-linolenic acid, which is the substrate for lipoxygenase (LOX) enzymes. The maize *LOX* family contains 13 members (*ZmLOX1–13*) (Ogunola *et al.*, 2017). Allene oxide cyclase (AOC) and oxophytodienoic acid reductase (OPR) catalyze the next two enzymatic reactions required for JA biosynthesis (Stenzel *et al.*, 2003). Jasmonate resistant 1 (JAR1) catalyzes the formation of a biologically active jasmonyl-isoleucine conjugate (Staswick and Tiryaki, 2004). Among all JA pathway genes, 12 (five *LOX*s, one *AOC*, four *OPR*s, and two *JAR*s) were differentially expressed after aphid infestation. *OPR1* (Zm00001d044908), *OPR2* (Zm00001d044906), and *JAR1b* (Zm00001d011377) were down-regulated in Abe2 compared with B73 at all time points. *LOX* (Zm00001d003533) expression was lower in both genotypes after aphid infestation, whereas *LOX11* (Zm00001d015852) was induced in Abe2 but relatively unchanged in B73 (Supplementary Table S5; Fig. 3A).

ET biosynthesis starts with methionine, which is converted to *S*-adenosyl-L-methionine (SAM) by SAM synthase (SAMS) (Wang *et al.*, 2002). SAM is then converted to 1-aminocyclopropane-1-carboxylic acid (ACC) by ACC synthase. Finally, ET is produced from ACC by ACC oxidase (ACO) (Houben and Van de Poel, 2019). Furthermore, the *ETHYLENE INSENSITIVE* (*EIN*) gene family in Arabidopsis (*Arabidopsis thaliana*) is required for ET signaling (Li *et al.*, 2015; Dolgikh *et al.*, 2019). Six ET pathway genes were differentially expressed in our dataset. For example, two SAMS-encoding genes (Zm00001d009146 and Zm00001d040697) had lower expression in Abe2 compared with B73. Three ACO-encoding genes showed significant expression variation: *ACO2* (Zm00001d020686) was down-regulated during aphid infestation except at 6 hpi in B73, *ACO15b* (Zm00001d024853) was down-regulated after aphid infestation except at 24 hpi in Abe2, and *ACO15a* (Zm00001d024843) was dramatically induced only in the resistant line Abe2. *EIN5* (Zm00001d016924) had reduced expression except at 6 hpi in Abe2 (Supplementary Table S5; Fig. 3B).

The isochorismate and phenylalanine ammonia lyase (PAL) pathways are both SA biosynthesis pathways (Dempsey *et al.*, 2011; Lefevere *et al.*, 2020). The gene encoding methyl esterase 3 (Zm00001d009398) was induced only in Abe2. The gene (Zm00001d021168) encoding UDP-glycosyltransferase, involved in SA glycosylation, was up-regulated at 6 hpi in both genotypes, but was down-regulated at 24 hpi in B73 (Supplementary Table S5; Fig. 3C).

Benzoxazinoid and volatile terpene biosynthesis are associated with aphid defense

BXs are important secondary metabolites in maize. Ten enzymes (BX1–BX9 and Igl1) catalyze the formation of DIMBOA-glc from indole-3-glycerol phosphate. Three homologous methoxytransferases, BX10–BX12, convert DIMBOA-glc to

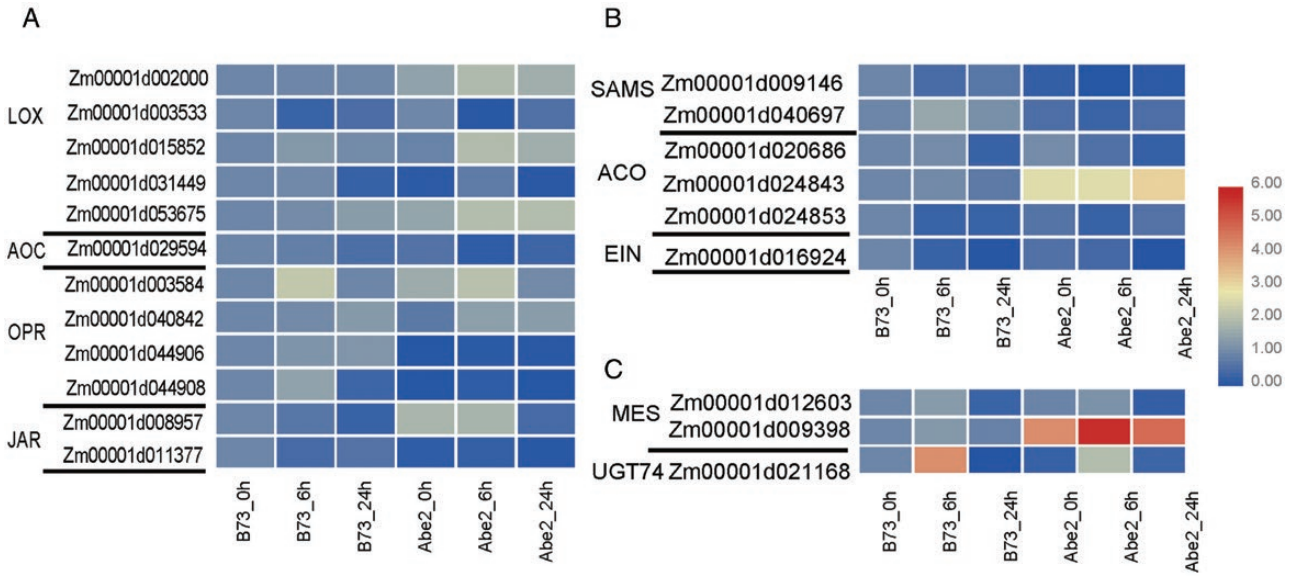

Fig. 3. Heatmap showing expression patterns of DEGs from hormone pathways in maize induced by *R. maidis* infestation. (A) JA pathway; (B) ET pathway; (C) SA pathway. Gene expression levels were transformed with $\log_2$ (FPKM+1). The B73-0h FPKM values were normalized to 1.

2-(2-hydroxy-4,7-dimethoxy-1,4-benzoxazin-3-one)-β-D-glucopyranose (HDMBOA-glc) (Meihls *et al.*, 2013). BX13 is a 2-oxoglutarate-dependent dioxygenase that catalyzes the conversion of DIMBOA-glc to 2-(2,4,7-trihydroxy-8-methoxy-1,4-benzoxazin-3-one)-β-D-glucopyranose (TRIMBOA-glc). BX14 is a methyltransferase that catalyzes the conversion of DIM_2BOA-glc to 2-(2-hydroxy-4,7,8-trimethoxy-1,4-benzoxazin-3-one)-β-D-glucopyranose (HDM_2BOA-glc) (Handrick *et al.*, 2016; Wisecaver *et al.*, 2017). Of the 14 annotated *BX*s, eight were differentially expressed in our dataset (Supplementary Table S6). *BX1* (Zm00001d048709) and *BX5* (Zm00001d048705) expression was much higher in Abe2 than in B73. Except for *BX1* and *BX5*, most of the BX biosynthesis-related genes were down-regulated at 6 hpi and up-regulated at 24 hpi in both genotypes (Supplementary Fig. S5).

Terpene synthases (TPSs) catalyze key steps in the formation of the terpene carbon skeleton (Chen *et al.*, 2011; Zhao *et al.*, 2021). To investigate whether the volatile terpene biosynthesis pathways respond to aphid feeding, we analyzed all the annotated *TPS*s in the maize genome. Of the 11 known *TPS* genes, we detected two in our transcriptome data: *TPS1* (Zm00001d002351) and *TPS7* (Zm00001d032230). Both were highly induced in Abe2 compared with B73, which suggests that TPS1 and TPS7 may have important roles in the response to aphid infestation (Supplementary Table S6).

Transcription factors involved in aphid defense

Among the TF genes differentially expressed between B73 and Abe2, the families most represented were NAC (27 TFs), WRKY (24 TFs), ethylene response factor (ERF; 21 TFs), basic leucine zipper (bZIP; 19 TFs), MYB (18 TFs), C2H2 (15 TFs), basic helix-loop-helix (bHLH; 14 TFs) and GRAS (12 TFs) (Fig. 4A). In total, 128 TF genes were differentially expressed between B73 and Abe2 under the control condition, and 120 and 111 TF genes were differentially expressed between B73 and Abe2 at 6 hpi and 24 hpi, respectively (Fig. 4B; Supplementary Table S7). Only 20 of the differentially expressed TF genes had the same pattern of regulation between the two lines at all time points, and most TF genes of the ERF, MYB, MYB-related, and NAC families showed higher expression in B73 than in Abe2 (Fig. 4C).

Identifying candidate aphid resistance genes by integrating QTL mapping and transcriptome data

To identify candidate genes for aphid resistance, we looked for co-localization of DEGs after aphid infestation in the QTL 2-LOD interval regions for aphid resistance on chromosome 6. Among the 28 genes detected in the QTL mapping, 10 were differentially expressed in Abe2 versus B73 after aphid infestation. Gene annotations indicated that three of these genes had functions related to pathways involved in stress responses (Table 2). Zm00001d035736 is homologous to Arabidopsis AT4G24290, which encodes a MAC/perforin (MACPF) domain-containing protein and is proposed to participate in the hypersensitive response as well as SA-mediated signaling pathways; Zm00001d035767 encodes a JA carboxyl methyltransferase (JMT) that is involved in the JA biosynthetic pathway; Zm00001d035751 is homologous to AT3G07370 and has functions in protein ubiquitination and the response to various stresses.

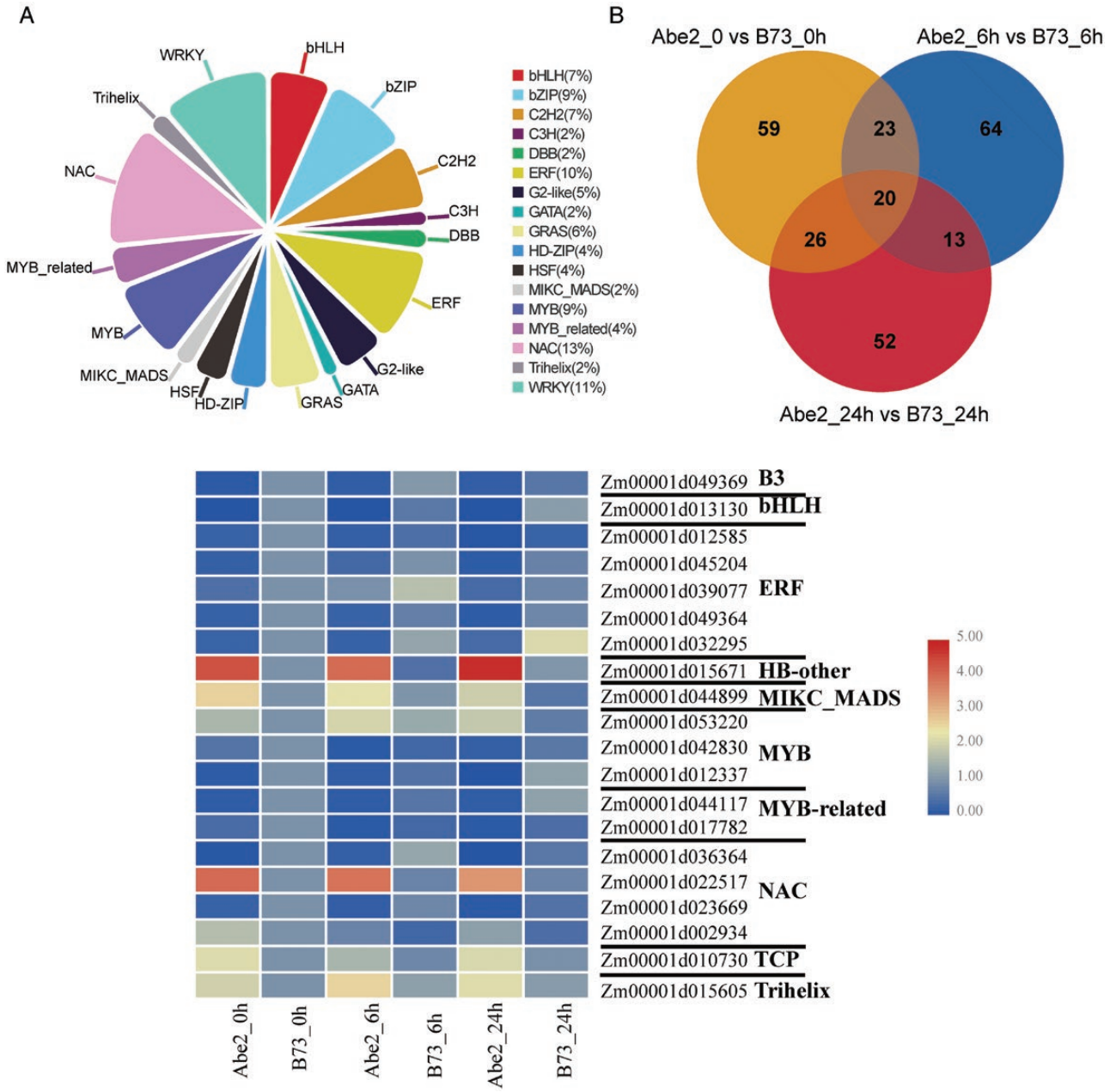

Fig. 4. Differentially expressed transcription factors after aphid infestation. (A) Distribution of differentially expressed transcription factors among different families. (B) Venn diagram of differentially expressed transcription factors between B73 and Abe2 at each examined time point of aphid infestation. (C) Heatmaps of common differentially expressed transcription factors. Gene expression levels were transformed with $\log_2$ (FPKM+1). The B73-0h FPKM values were normalized to 1.

To explore whether the loci in the QTL affect gene expression, we identified the physical locations of variant SLAF markers flanking the QTL *qRTA6* and the genes near the markers, and found that Marker13341795 was located in the Zm00001d035737 genomic region and Marker13675381 was located in the Zm00001d035757 genomic region, which may suggest a direct genetic linkage between the expression of these two genes and aphid resistance. Furthermore, we mined the sequence variation of candidate genes in the QTL between the two parents from our transcriptome sequencing data. Zm00001d035731 has nine SNPs in the genomic region (including exonic, intronic, and untranslated regions); Zm00001d035736 has nine SNPs in the genomic region; Zm00001d035737 has 19 SNPs in the genomic region; Zm00001d035741 has 12 SNPs in the genomic region, Zm00001d035751 has 10 SNPs in the genomic region; Zm00001d035752 has three SNPs in the genomic region; Zm00001d035757 has 57 SNPs in the genomic region;

Table 2. List of DEGs between B73 and Abe2 within the *qRTA-6* confidence intervals

Gene ID	Position (bp)	Arabidopsis ortholog	Gene name	Annotation	B73_ 0h	B73_ 6h	B73_ 24h	Abe2_ 0h	Abe2_ 6h	Abe2_ 24h
Zm00001d035731	43838390–43846359	AT5G22450	*SCS1*	Saga complex submit 1	4.55	8.19	5.92	6.67	8.35	5.34
Zm00001d035736	44288172–44292160	AT4G24290	*MACPF*	MAC/perforin domain-containing protein	3.02	6.28	2.59	6.31	9.43	3.33
Zm00001d035737	44300291–44304215	AT1G80380	*GLYK*	Glycerate kinase activity	111.55	122.79	133.37	126.23	170.02	188.62
Zm00001d035741	44431908–44435502	AT4G17530	*RAB1C*	RAB GTPase homolog 1C	7.30	6.63	7.99	13.77	13.94	13.30
Zm00001d035751	45350374–45356168	AT3G07370	*CHIP*	Carboxyl terminus of Hsc70-interacting protein	4.31	6.77	5.72	8.26	11.02	5.99
Zm00001d035752	45356441–45358855	AT2G39990	*EIF3*	Translation initiation factor activity	23.04	17.93	26.16	29.03	13.10	50.86
Zm00001d035757	45715257–45726111	AT1G22860	*VPS3*	Vesicle-mediated transport	1.95	2.14	1.73	7.41	2.45	5.50
Zm00001d035759	46086182–46086394	AT3G48660	*DUF3339*	Protein of unknown function	30.86	20.34	38.35	29.19	38.01	92.51
Zm00001d035761	46130267–46133225	AT5G13120	*CYP20-2*	Cyclophilin 20-2	101.29	103.50	74.35	93.94	140.13	254.57
Zm00001d035767	46577784–46579578	AT1G19640	*JMT*	Jasmonic acid carboxyl methyltransferase	3.67	1.90	31.06	8.76	1.53	115.02

Zm00001d035759 has two SNPs in the genomic region; and Zm00001d035761 has two SNPs in the genomic region (Supplementary Table S8). These sequence variations could be related to the function of the genes or differential gene expression.

To validate the RNA-seq results, we selected nine genes, related to secondary metabolism (Zm00001d048703, Zm00001d048705, Zm00001d027472, and Zm00001d014865) and phytohormones (Zm00001d020409, Zm00001d035767, and Zm00001d015464), as well as two TFs (Zm00001d015743 and Zm00001d049543), for RT–qPCR. The overall RT–qPCR expression patterns of these genes were consistent with the expression patterns observed by RNA-seq (Supplementary Fig. S6; Supplementary Table S9).

Identifying differentially accumulated metabolites in B73 and Abe2 after aphid infestation through metabolome analysis

To explore the metabolic changes that occur following aphid infestation, we conducted untargeted metabolome analysis of B73 and Abe2 leaves at 24 hpi, with uninfested leaves serving as controls. The comparisons included B73-24h versus B73-0h, Abe2-24h versus Abe2-0h, Abe2-0h versus B73-0h, and Abe2-24h versus B73-24h. Principal component analysis revealed a high level of consistency within each biological replicate group, and separation between the two genotypes and between the infested and control groups (Supplementary Fig. S7A). Partial least squares discriminant analysis also revealed significant biochemical changes among the different sample groups (Supplementary Fig. S7B), which suggested that VIP values could be used to screen the DAMs.

Based on VIP>1 and $P<0.05$, we identified many DAMs in the different comparisons, including 157 up-regulated and 122 down-regulated DAMs in B73-24h versus B73-0h, 160 up-regulated and 182 down-regulated DAMs in Abe2-24h versus Abe2-0h, 206 up-regulated and 152 down-regulated DAMs in Abe2-0h versus B73-0h, and 201 up-regulated and 170 down-regulated DAMs in Abe2-24h versus B73-24h (Fig. 5A). Furthermore, 52 DAMs were common to all four comparisons (Fig. 5B).

According to the HMDB database annotation, the identified DAMs in maize leaves responsive to aphid infestation were mainly classified into 13 classes. The DAMs were mainly organoheterocyclic compounds, phenylpropanoids and polyketides, organic acids and derivative, lipids and their derivatives, and benzenoids (Supplementary Fig. S8).

KEGG analysis of DAMs in B73 and Abe2 after aphid infestation

To identify metabolites that contribute to aphid resistance, we subjected the DAMs to KEGG analysis. The significantly enriched KEGG terms are shown in Fig. 6. The DAMs were enriched in many pathways, including vitamin B6 metabolism, flavonoid biosynthesis, ABC transporters, glutathione metabolism, and tryptophan metabolism. The top enriched term in the four comparisons was flavonoid metabolism, including the flavonoid biosynthesis and flavone and flavonol biosynthesis pathways, indicating that flavonoid metabolism is important for aphid resistance in maize. The number of differentially expressed flavonoids between Abe-0h and B73-0h was 26, of which 18 (three flavanones, six flavones, and nine flavonoid glycosides) increased and eight (one flavone, six flavonoid

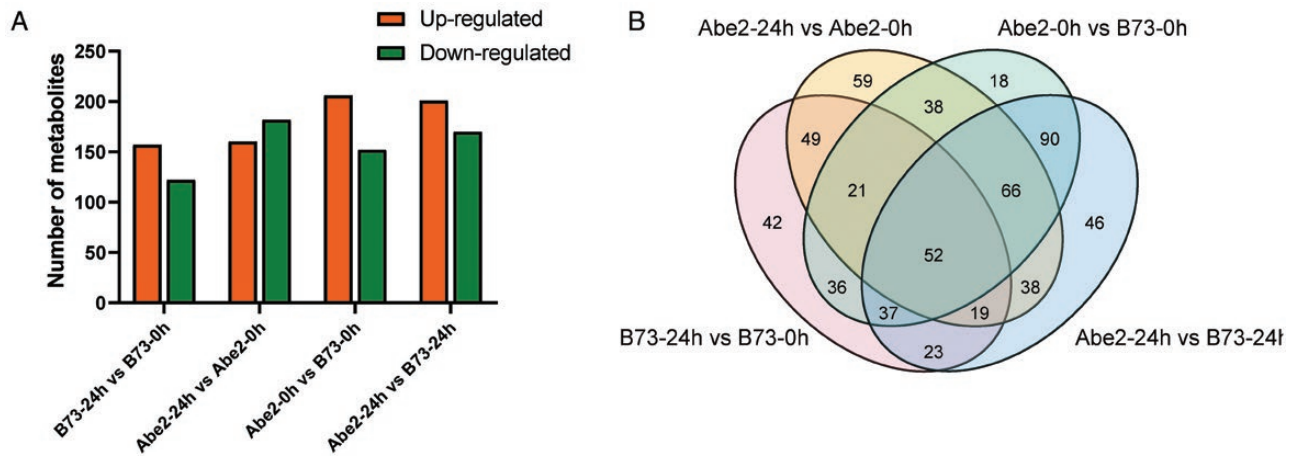

Fig. 5. Analysis of DAMs in maize upon *R. maidis* infestation. (A) Numbers of up-regulated and down-regulated DAMs in different pairs of comparisons. (B) Venn diagram of DAMs in different comparisons.

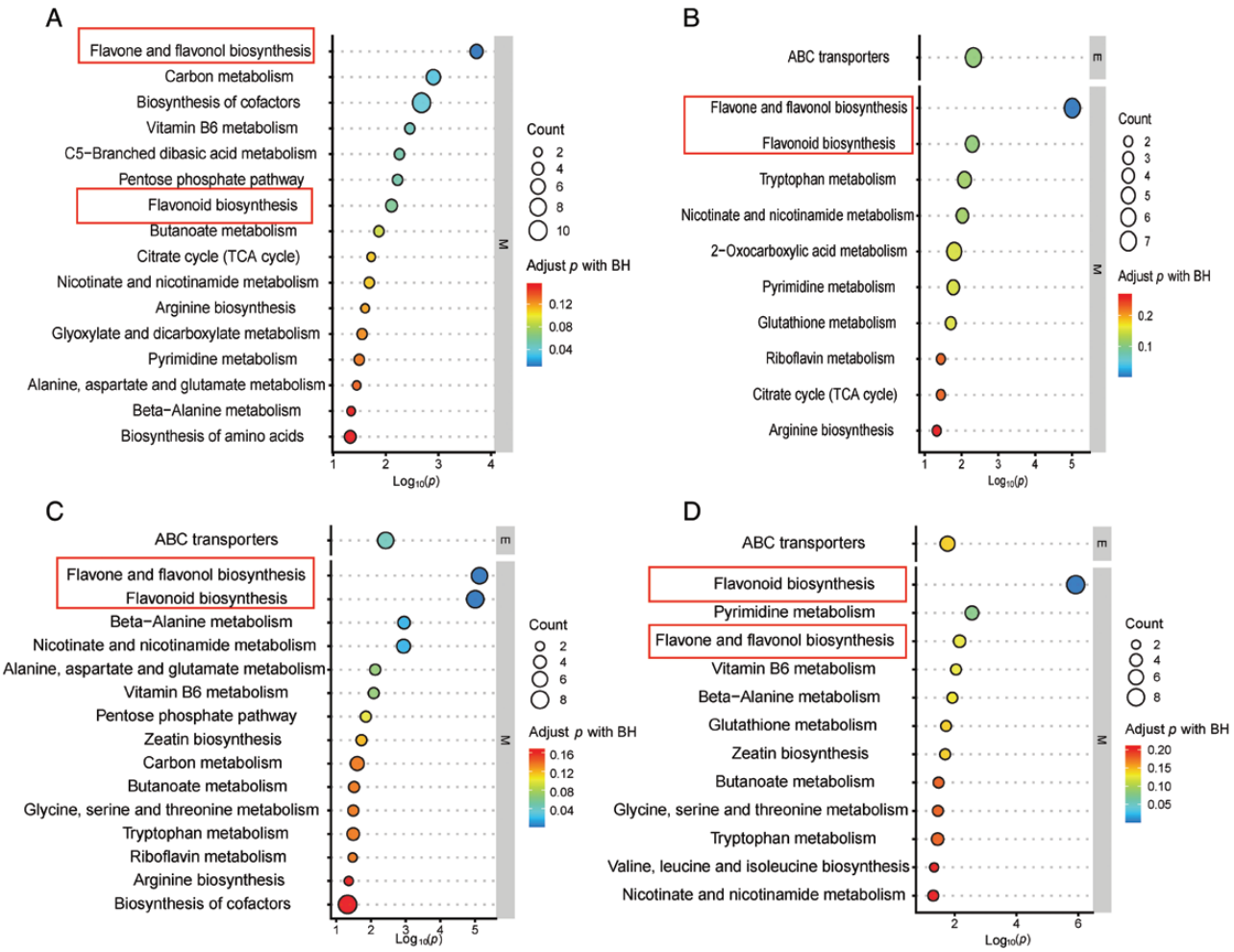

Fig. 6. KEGG enrichment analysis of DAMs under *R. maidis* infestation in different comparisons. (A) KEGG pathways significantly enriched in B73-24h versus B73-0h. (B) KEGG pathways significantly enriched in Abe2-24h versus Abe2-0h. (C) KEGG pathways significantly enriched in Abe2-0h versus B73-0h. (D) KEGG pathways significantly enriched in Abe2-24h versus B73-24h. The *P*-value is further corrected by multiple testing, applying the Benjamini–Hochberg (BH) method to obtain the FDR value.

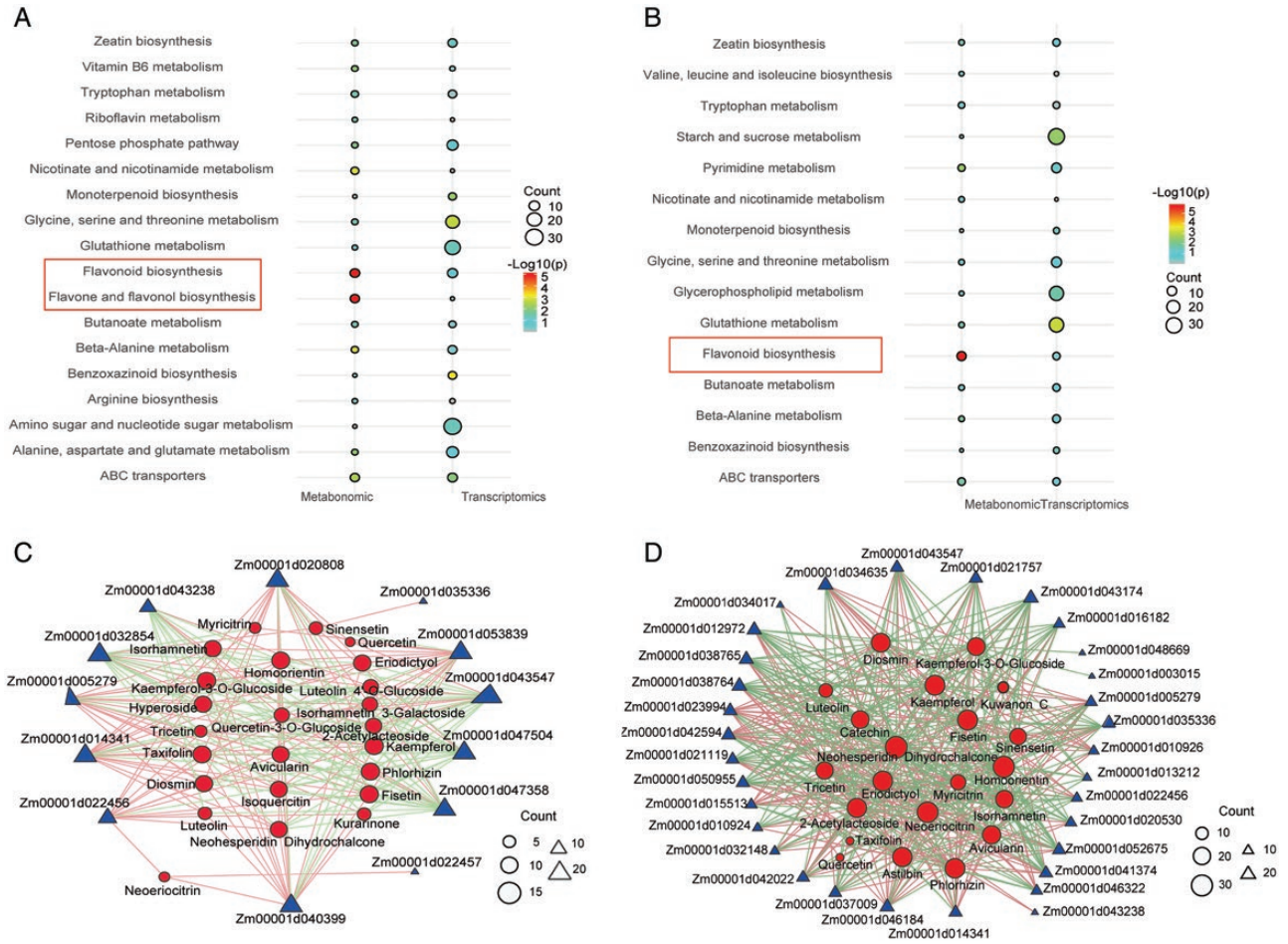

Fig. 7. Correlation analysis of DEGs and DAMs of maize leaves after *R. maidis* infestation. (A) KEGG analysis of DEGs and DAMs that were enriched in the same pathway in Abe2-0h vsversus B73-0h. (B) KEGG analysis of DEGs and DAMs that were enriched in the same pathway in Abe2-24h versus B73-24h. (C) Correlation network of DEGs and DAMs in Abe2-0h versus B73-0h. (D) Correlation network of DEGs and DAMs in Abe2-24h versus B73-24 h. In (C, D), each node represents a gene or metabolite; blue triangles indicate genes and red circles indicate metabolites. The different node (circle/triangle) sizes represent the degree, which is the most direct measurement to describe the node centrality in the network analysis. The connectivity (degree) of a node n refers to the number of edges linked to n. The node-to-node connections (edges) represent the weighted Pearson correlation coefficient values for each gene and metabolite pair. Red and green lines represent positive and negative correlations, respectively.

glycosides, and one *O*-methylated flavonoids) decreased. In the comparison between Abe-24h versus Abe-0h, four flavonoids (2-acetylacteoside, luteolin 4′-O-glucoside, 4,5,7-trihydroxy-3,6-dimethoxyflavone, and didymin) were up-regulated, only 2-acetylacteoside was not induced in B73, and a comparison between B73-24h and B73-0h showed that six flavonoids (diosmin, rhoifolin, kaempferol, fisetin, myricitrin, and myricetin) decreased. However, only rhoifolin was not induced in Abe2 (Supplementary Table S10). These results suggest that 2-acetylacteoside and rhoifolin may potentially associate with the aphid resistance of Abe2.

Integrated transcriptomic and metabolomic analyses of maize leaves after aphid infestation

To further investigate the regulatory network in maize in response to aphid infestation, correlation analysis was performed between our transcriptomic and metabolomic data. First, combined KEGG analyses of DEGs and DAMs were conducted. In Ab2-0h versus B73-0h, the most enriched KEGG pathway from the transcriptome and metabolome was flavonoid biosynthesis, and the second most enriched pathway was flavone and flavonol biosynthesis. Similarly, flavonoid biosynthesis was the most enriched pathway in Ab2-24h versus B73-24h. The other enriched pathways were zeatin biosynthesis, tryptophan metabolism, glycine, serine, and threonine metabolism, glutathione metabolism, BX biosynthesis and ABC transporters (Fig. 7A, B). To further explore the relationship between the DEGs and DAMs enriched in flavonoid biosynthesis in Abe2 and B73, we conducted a correlation analysis and generated a co-expression network of DEGs and DAMs (R>0.8 or R<–0.8, P<0.05; Fig. 7C, D; Supplementary Table S11). Zm00001d053839 was significantly and positively correlated with quercetin (R=0.87) in Ab2-0h versus B73-0h; Zm00001d034635 had

a strong positive correlation with kaempferol (R=0.97) in Ab2-24h versus B73-24h. An association analysis revealed a higher relativity between quantitative changes of flavonoids and transcripts and identified the key regulatory genes such as Zm00001d053839 and Zm00001d034635, suggesting that these genes might be involved in the regulation of flavonoid accumulation in response to aphid infestation.

Profiles of the flavonoid biosynthesis-related genes and metabolites responsive to aphid infestation

Our combined transcriptomic and metabolomic analyses suggested that flavonoid metabolism is important for aphid resistance in maize. To demonstrate the effects of aphid infestation on genes and metabolites in the flavonoid pathway, we analyzed the main DEGs and DAMs involved in this pathway in B73 and Abe2 at 0 hpi and 24 hpi (Fig. 8; Supplementary Table S12). We identified seven DEGs related to flavonoid biosynthesis in Abe2 and B73: two genes encoding phenylalanine ammonia lyase (PAL, Zm00001d017275 and Zm00001d051163) and two genes encoding 4-coumarate-CoA ligase (4CL, Zm00001d051529 and Zm00001d015459) were down-regulated in Abe2 at 24 hpi; *Chalcone synthase* (*CHS*, Zm00001d052675) and *Chalcone isomerase 3* (*CHI3*, Zm00001d012972) were significantly down-regulated in Abe2 at both time points; and *Chalcone isomerase* (*CHI1*, Zm00001d034635) was significantly up-regulated in Abe2 at both time points. Moreover, four downstream metabolites involved in flavonoid biosynthesis (luteolin, eriodictyol, quercetin, and kaempferol) were significantly up-regulated in Abe2 at both time points (Fig. 8; Supplementary Table S10). These results suggest that the DEGs and DAMs related to flavonoid biosynthesis may coordinately respond to aphid infestation in maize.

Discussion

Many QTLs related to aphid resistance have been identified by linkage mapping (Butrón *et al.*, 2010; Meihls *et al.*, 2013; Betsiashvili *et al.*, 2015); however, fine-mapping of causative genes requires the time-consuming establishment of large segregating populations. Transcriptome analysis has shown the power to facilitate the identification of candidate genes that function in the response to insect stress, and can limit the range of candidate genes detected by QTL mapping (X. Wu *et al.*, 2020). This integrated approach has been used in different plant species to detect the genes controlling agronomic traits (Odilbekov *et al.*, 2019; Yao *et al.*, 2020). Here, we used a similar method to identify candidate genes for resistance during aphid infestation. Field observation and screening revealed that Abe2 has significantly better aphid resistance than B73 (Fig. 1). Using the B73×Abe2 RIL population, we identified a main-effect QTL, *qRTA6*, on chromosome 6, associated with aphid resistance. The chromosomal location of *qRTA6* (Fig. 2; Table 2) differed from that of previously reported candidate aphid-resistance genes in maize (Butrón *et al.*, 2010). Further genetic mapping could uncover additional aphid-resistance genes and mechanisms in maize.

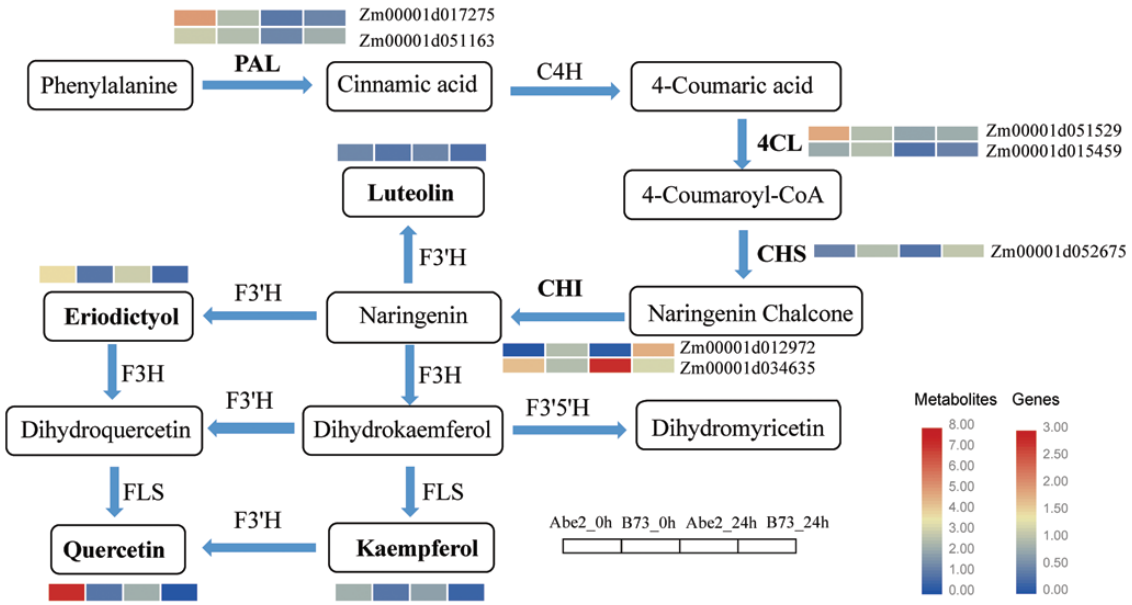

Fig. 8. Expression profiles of DEGs and DAMs involved in flavonoid metabolism in Abe2 and B73 in response to aphid infestation. PAL, phenylalanine ammonia lyase; C4H, cinnamate-4-hydroxylase; 4CL, 4-coumarate-CoA ligase; CHS, chalcone synthase; CHI, chalcone isomerase; F3H, flavanone 3-hydroxylase; F3′H, flavonoid 3′-hydroxylase; F3′5 ′H, flavonoid 3′, 5′-hydroxylase; FLS, flavonol synthase. The gene expression and metabolite accumulation levels of B73-0h were normalized to 1.

Given that resistance genes may respond quickly during aphid infestation, we conducted RNA-seq analysis at three time points during aphid infestation (0, 6, and 24 hpi) to reveal potential candidate genes. Plant hormone signal transduction was among the most enriched pathways of the DEGs. JA, SA, and ET are important signaling molecules during defense against insects. Genes involved in the biosynthesis of these phytohormones showed differential responses to aphid infestation between the resistant line Abe2 and the susceptible line B73 (Fig. 3; Supplementary Table S5), which confirmed the importance of phytohormones in aphid resistance.

Aphid infestation caused numerous metabolite changes in maize. BX biosynthesis was the most or second most enriched pathway among the DEGs for all time points, and many BX biosynthesis genes had higher expression in Abe2 than in B73 upon aphid infestation. BX1 is the initial enzyme in the BX biosynthesis pathway, and the high *BX1* expression in the aphid-resistant line Mo17 likely causes its high BX content (Zheng *et al.*, 2015). Here, the high expression of BX-related genes in Abe2 likely contributed to the higher resistance of this line to *R. maidis* (Supplementary Fig. S5; Supplementary Table S6). In addition to BX biosynthesis, terpenoid and polyketide metabolism was also significantly enriched at all time points. *TPS1* and *TPS7*, which encode enzymes catalyzing the formation of certain terpenes, showed induced expression following *R. maidis* infestation; *TPS7* had higher expression in Abe2 than in B73 at 24 hpi (Supplementary Table S6). These data suggest that BX- and terpene-related genes may contribute to aphid resistance. For the transcriptome analysis, the DEGs involved in the pathway of BXs and terpenes were significantly differentially expressed in B73 versus Abe2. However, for the metabolome analysis, we did not map any direct products associated with these pathways. It is possible that relatively fewer metabolites are measured by non-targeted metabolic analysis compared with RNA-seq analysis, or that those metabolites are the product of co-regulation by a range of genes, and the changes in the expression of individual genes are not sufficient to cause differential metabolite accumulation.

Feeding by herbivorous insects triggers changes in TF gene expression, which in turn affects the expression of downstream defense-response genes. TFs are key regulators of insect resistance. For instance, OsMYB30, an R2R3 MYB TF, confers resistance to the brown planthopper (*Nilaparvata lugens*) in rice (He *et al.*, 2020), and the TF BrERF11b significantly enhances plant resistance to the green peach aphid (*Myzus persicae*) and the tobacco cutworm (*Spodoptera litura*) (J. Wu *et al.*, 2020). In our study, *R. maidis* infestation altered the expression of 257 TF genes in Abe2 and B73, and 20 TFs were differentially expressed between Abe2 and B73 at all time points of the experiment. Among these 20 TFs, most of the ERF, MYB, MYB-related and NAC TFs had higher expression in B73 than in Abe2 (Fig. 4; Supplementary Table S7).

Our combined transcriptomic and metabolomic analyses revealed that DEGs and DAMs involved in flavonoid biosynthesis were significantly enriched in the aphid-resistant line Abe2 compared with the susceptible line B73 (Fig. 7A, B). Flavonoid biosynthesis, which occurs downstream of phenylpropane metabolism, has been widely reported to have protective functions in plant tolerance to different biotic and abiotic stresses (Falcone Ferreyra *et al.*, 2012). PAL is the first enzyme in phenylpropane metabolism. Two *PAL* genes were induced in Abe2 and B73 at 0 hpi relative to 24 hpi. 4CL catalyzes the production of 4-coumaroyl-CoA, which is a substrate for CHS, in the last step of phenylpropane metabolism. Two *4CL* genes were up-regulated in Abe2 and B73 leaves at 0 hpi compared with 24 hpi. CHS converts one molecule of 4-coumaroyl-CoA to naringenin chalcone, which is the substrate for CHI, and then converts naringenin chalcone to naringenin (Li *et al.*, 2021). The *CHS* gene and two *CHI* genes were up-regulated in Abe2-24h versus Abe2-0h and in B73-24h versus B73-0h. Quercetin, kaempferol, and myricetin, downstream metabolites in flavonoid biosynthesis, are involved in scavenging reactive oxygen species (Belinha *et al.*, 2007). Flavonoids, including luteolin, eriodictyol, quercetin, and kaempferol were more abundant in the resistant line Abe2 (Fig. 8), indicating that reactive oxygen species scavenging may participate in the defensive response to aphids in maize.

By integrating the DEGs from RNA-seq with QTL mapping data, we identified three candidate aphid-resistance genes in maize (Table 2). Zm00001d035736 encodes a MACPF domain-containing protein, which is involved in the hypersensitive response. The Arabidopsis gene *CAD1* encodes a MACPF domain-containing protein, which negatively controls SA-mediated programmed cell death in plant immunity (Morita-Yamamoto *et al.*, 2005). Zm00001d035767 encodes a JMT that catalyzes the formation of methyl jasmonate from JA (Seo *et al.*, 2001). JMT regulates the level of active JA, which functions in the defense response to diverse external environmental stresses, including insect damage (Qi *et al.*, 2016). It has been reported that the flavonoid accumulation in licorice (*Glycyrrhiza uralensis*) cells could be enhanced by adding methyl jasmonate (Li *et al.*, 2020). Therefore, we speculate that the plant hormone JA might modulate the flavonoid biosynthesis in maize response to aphids. Zm00001d035751 encodes a carboxyl terminus of Hsc70-interacting protein (CHIP), which is an E3 ubiquitin ligase involved in protein ubiquitination. *CHIP* genes are induced by several abiotic stresses, including cold, heat, and salt (Yan *et al.*, 2003). *chip* mutants appear normal under optimal growth conditions but are hypersensitive to heat, salt, and oxidative stresses (Zhou *et al.*, 2014). To conclude, the candidate aphid-resistance genes identified here may be valuable resources for breeding for increased resistance in maize.

Supplementary data

The following supplementary data are available at *JXB* online.

Table S1. Primer sequences used for RT–qPCR analysis.

Table S2. List of genes located within the *qRTA6* region.

Table S3. Statistics of RNA-seq reads mapped to the B73_V4 reference genome assembly for all samples.

Table S4. Statistics of DEGs in B73 and Abe2 before and after aphid infestation.

Table S5. Expression levels of the DEGs involved in phytohormone pathways between B73 and Abe2.

Table S6. Expression levels of the DEGs involved in BX and terpene biosynthesis between B73 and Abe2.

Table S7. Transcription factor genes differentially expressed between B73 and Abe2.

Table S8. Sequence variation of candidate genes in the QTL between B73 and Abe2 from the transcriptome sequencing data.

Table S9. Comparison of RNA-seq and RT–qPCR data of nine selected genes.

Table S10. DAMs involved in flavonoid biosynthesis after *R. maidis* infestation between B73 and Abe2.

Table S11. Correlated DEGs and DAMs involved in flavonoid biosynthesis between B73 and Abe2.

Table S12. DEGs involved in flavonoid biosynthesis after *R. maidis* infestation between B73 and Abe2.

Fig. S1. Scoring system for *R. maidis* resistance levels based on aphid coverage area on maize individuals.

Fig. S2. Pearson's correlations between three biological replicates for each of six samples.

Fig. S3.Venn diagrams of DEGs during *R. maidis* infestation.

Fig. S4. KEGG enrichment analysis of DEGs after *R. maidis* infestation between different comparisons.

Fig. S5. Relative expression changes of DEGs involved in benzoxazinoid biosynthesis after *R. maidis* infestation.

Fig. S6. Comparison of expression levels of nine DEGs in RNA-seq and RT–qPCR analyses.

Fig. S7. Overview of metabolome analysis of Abe2 and B73 before and after *R. maidis* infestation.

Fig. S8. Categories of DAMs in Abe2 and B73 after *R. maidis* infestation.

Author contributions

WT, WK, XC, and LP conceived and designed the study; WC and WK designed the experiments; WL, SJ, and ZY conducted the experiments; TZ, LJ, and HS analyzed the data; WT and WK wrote the paper; XC and LP edited the paper.

Conflict of interest

All the authors declare that they have no competing financial interests or personal relationships that could influence the work reported in this paper.

Funding

This work was supported by the National Key Research and Development Program of China (2022YFD1201803), Anhui Provincial Major Science and Technology Project (202203a06020005), the National Natural Science Foundation of China (32171954 and 32202322), and Anhui Provincial Natural Science Foundation (2208085QC86 and 2008085QC121).

Data availability

Raw reads of RNA-seq have been deposited in the NCBI Sequence Read Archive (https://www.ncbi.nlm.nih.gov/sra) under accession number PRJNA871985. All other supporting the findings of this study are included within the paper and within its supplementary data published online.

References

Ahmad S, Veyrat N, Gordon-Weeks R, *et al*. 2011. Benzoxazinoid metabolites regulate innate immunity against aphids and fungi in maize. Plant Physiology **157**, 317–327.

Bai Y, Yang C, Halitschke R, Paetz C, Kessler D, Burkard K, Gaquerel E, Baldwin IT, Li D. 2022. Natural history-guided omics reveals plant defensive chemistry against leafhopper pests. Science **375**, eabm2948.

Belinha I, Amorim MA, Rodrigues P, Freitas V, Moradas-Ferreira P, Mateus N, Costa V. 2007. Quercetin increases oxidative stress resistance and longevity in *Saccharomyces cerevisiae*. Journal of Agricultural and Food Chemistry **55**, 2446–2451.

Berens ML, Berry HM, Mine A, Argueso CT, Tsuda K. 2016. Evolution of hormone signaling networks in plant defense. Annual Review of Phytopathology **55**, 401–425.

Betsiashvili M, Ahern KR, Jander G. 2015. Additive effects of two quantitative trait loci that confer *Rhopalosiphum maidis* (corn leaf aphid) resistance in maize inbred line Mo17. Journal of Experimental Botany **66**, 571–578.

Brault V, Uzest M, Monsion B, Jacquot E, Blanc S. 2010. Aphids as transport devices for plant viruses. Comptes Rendus Biologies **333**, 524–538.

Butrón A, Chen YC, Rottinghaus GE, Mcmullen MD. 2010. Genetic variation at *bx1* controls DIMBOA content in maize. Theoretical and Applied Genetics **120**, 721–734.

Carena MJ, Glogoza P. 2004. Resistance of maize to the corn leaf aphid: a review. Maydica **49**, 241–254.

Chapman KM, Marchi-Werle L, Hunt TE, Heng-Moss TM, Louis J. 2018. Abscisic and jasmonic acids contribute to soybean tolerance to the soybean aphid (*Aphis glycines Matsumura*). Scientific Reports **8**, 15148.

Chen C, Chen H, Huang S, Jiang T, Li P. 2021. Volatile DMNT directly protects plants against *Plutella xylostella* by disrupting peritrophic matrix barrier in midgut. eLife **10**, e63938.

Chen C, Rui X, Hao C, He Y. 2018. TBtools: an integrated toolkit developed for interactive analyses of big biological data. Molecular Plant **13**, 1194–1202.

Chen F, Tholl D, Bohlmann J, Pichersky E. 2011. The family of terpene synthases in plants: a mid-size family of genes for specialized metabolism that is highly diversified throughout the kingdom. The Plant Journal **66**, 212–229.

Chen H, Chen C, Huang S, *et al*. 2022. Inactivation of RPX1 in *Arabidopsis* confers resistance to *Plutella xylostella* through the accumulation of the homoterpene DMNT. Plant, Cell and Environment **46**, 946–961.

Costarelli A, Bianchet C, Ederli L, Salerno G, Piersanti S, Rebora M, Pasqualini S. 2019. Salicylic acid induced by herbivore feeding antagonizes jasmonic acid mediated plant defenses against insect attack. Plant Signaling & Behavior **15**, 1704517.

Dempsey DA, Vlot AC, Wildermuth MC, Klessig DF. 2011. Salicylic acid biosynthesis and metabolism. The Arabidopsis Book **9**, e0156.

Dolgikh VA, Pukhovaya EM, Zemlyanskaya EV. 2019. Shaping ethylene response: the role of EIN3/EIL1 transcription factors. Frontiers in Plant Science **10**, 1030.

Erb M, Reymond P. 2019. Molecular interactions between plants and insect herbivores. Annual Review of Plant Biology **70**, 527–557.

Falcone Ferreyra M, Rius SP, Casati P. 2012. Flavonoids: biosynthesis, biological functions, and biotechnological applications. Frontiers in Plant Science **3**, 222.

Handrick V, Robert CAM, Ahern KR, *et al*. 2016. Biosynthesis of 8-*O*-methylated benzoxazinoid defense compounds in maize. The Plant Cell **28**, 1682–1700.

He J, Liu Y, Yuan D, *et al*. 2020. An R2R3 MYB transcription factor confers brown planthopper resistance by regulating the phenylalanine ammonia-lyase pathway in rice. Proceedings of the National Academy of Sciences, USA **117**, 271–277.

Houben M, Van de Poel B. 2019. 1-aminocyclopropane-1-carboxylic acid oxidase (ACO): the enzyme that makes the plant hormone ethylene. Frontiers in Plant Science **10**, 695.

Jiao Y, Peluso P, Shi J, *et al*. 2017. Improved maize reference genome with single-molecule technologies. Nature **546**, 524–527.

Jin J, Tian F, Yang D-C, Meng Y-Q, Kong L, Luo J, Gao G. 2017. PlantTFDB 4.0: toward a central hub for transcription factors and regulatory interactions in plants. Nucleic Acids Research **45**, D1040–D1045.

Kettles GJ, Drurey C, Schoonbeek HJ, Maule AJ, Hogenhout SA. 2013. Resistance of *Arabidopsis thaliana* to the green peach aphid, *Myzus persicae*, involves camalexin and is regulated by microRNAs. New Phytologist **198**, 1178–1190.

Kloth KJ, Wiegers GL, Busscher-Lange J, van Haarst JC, Kruijer W, Bouwmeester HJ, Dicke M, Jongsma MA. 2016. AtWRKY22 promotes susceptibility to aphids and modulates salicylic acid and jasmonic acid signalling. Journal of Experimental Botany **67**, 3383–3396.

Lefevere H, Bauters L, Gheysen G. 2020. Salicylic acid biosynthesis in plants. Frontiers in Plant Science **11**, 338.

Li B, Fan R, Sun G, *et al*. 2021. Flavonoids improve drought tolerance of maize seedlings by regulating the homeostasis of reactive oxygen species. Plant and Soil **461**, 389–405.

Li W, Ma M, Feng Y, Li H, Wang Y, Ma Y, Li M, An F, Guo H. 2015. EIN2-directed translational regulation of ethylene signaling in Arabidopsis. Cell **163**, 670–683.

Li Y, Chen X, Wang J, Zou G, Wang L, Li X. 2020. Two responses to MeJA induction of R2R3-MYB transcription factors regulate flavonoid accumulation in *Glycyrrhiza uralensis* Fisch. PLoS One **15**, e0236565.

Liang D, Chen M, Qi X, Xu Q, Zhou F, Chen X. 2016. QTL mapping by SLAF-seq and expression analysis of candidate genes for aphid resistance in cucumber. Frontiers in Plant Science **7**, 1000.

Liu C, Zhou Q, Dong L, Wang H, Liu F, Weng J, Li X, Xie C. 2016. Genetic architecture of the maize kernel row number revealed by combining QTL mapping using a high-density genetic map and bulked segregant RNA sequencing. BMC Genomics **17**, 1–10.

Loreto F, D'Auria S. 2021. How do plants sense volatiles sent by other plants? Trends in Plant Science **27**, 29–38.

Louis J, Basu S, Varsani S, Castano-Duque L, Jiang V, Williams WP, Felton GW, Luthe DS. 2015. Ethylene contributes to *maize insect resistance1*-mediated maize defense against the phloem sap-sucking corn leaf aphid. Plant Physiology **169**, 313–324.

Love MI, Huber W, Anders S. 2014. Moderated estimation of fold change and dispersion for RNA-seq data with DESeq2. Genome Biology **15**, 550.

Ma F, Yang X, Shi Z, Miao X. 2020. Novel crosstalk between ethylene- and jasmonic acid-pathway responses to a piercing–sucking insect in rice. New Phytologist **225**, 474–487.

Mccouch S, Cho Y, Yano M, Paul E, Blinstrub M, Morishima H, Mccouch S, Cho Y, Paul E, Morishima H. 1997. Report on QTL nomenclature. Rice Genetics Newsletter **14**, 11–13.

Meihls LN, Handrick V, Glauser G, *et al*. 2013. Natural variation in maize aphid resistance is associated with 2,4-dihydroxy-7-methoxy-1,4-benzoxazin-3-one glucoside methyltransferase activity. The Plant Cell **25**, 2341–2355.

Meihls LN, Kaur H, Jander G. 2012. Natural variation in maize defense against insect herbivores. Cold Spring Harbor Symposia on Quantitative Biology **77**, 269–283.

Morita-Yamamoto C, Tsutsui T, Sato M, *et al*. 2005. The *Arabidopsis* gene *CAD1* controls programmed cell death in the plant immune system and encodes a protein containing a MACPF domain. Plant and Cell Physiology **46**, 902–912.

Morkunas I, Mai VC, Gabryś B. 2011. Phytohormonal signaling in plant responses to aphid feeding. Acta Physiologiae Plantarum **33**, 2057–2073.

Mu X, Dai Z, Guo Z, Zhang H, Yang J, Gan X, Li J, Liu Z, Tang J, Gou M. 2021. Systematic dissection of disease resistance to southern corn rust by bulked-segregant and transcriptome analysis. The Crop Journal **10**, 426–435.

Odilbekov F, He X, Armonienė R, Saripella GV, Chawade A. 2019. QTL mapping and transcriptome analysis to identify differentially expressed genes induced by Septoria tritici blotch disease of wheat. Agronomy **9**, 510.

Ogunola OF, Hawkins LK, Mylroie E, Kolomiets MV, Borrego E, Tang JD, Williams WP, Warburton ML. 2017. Characterization of the maize lipoxygenase gene family in relation to aflatoxin accumulation resistance. PLoS One **12**, e0181265.

Pingault L, Varsani S, Palmer N, Ray S, Williams WP, Luthe DS, Ali JG, Sarath G, Louis J. 2021. Transcriptomic and volatile signatures associated with maize defense against corn leaf aphid. BMC Plant Biology **21**, 138.

Qi J, Li J, Han X, Li R, Wu J, Yu H, Hu L, Xiao Y, Lu J, Lou Y. 2016. Jasmonic acid carboxyl methyltransferase regulates development and herbivory-induced defense response in rice. Journal of Integrative Plant Biology **58**, 564–576.

Qi J, Malook SU, Shen G, Gao L, Zhang C, Li J, Zhang J, Wang L, Wu J. 2018. Current understanding of maize and rice defense against insect herbivores. Plant Diversity **40**, 189–195.

Richter A, Schaff C, Zhang Z, *et al*. 2016. Characterization of biosynthetic pathways for the production of the volatile homoterpenes DMNT and TMTT in *Zea mays*. The Plant Cell **28**, 2651–2665.

Schnable PS, Ware D, Fulton RS, *et al*. 2009. The B73 maize genome: complexity, diversity, and dynamics. Science **326**, 1112–1115.

Seo HS, Song JT, Cheong JJ, Lee YH, Lee YW, Hwang I, Lee JS, Choi YD. 2001. Jasmonic acid carboxyl methyltransferase: a key enzyme for jasmonate-regulated plant responses. Proceedings of the National Academy of Sciences, USA **98**, 4788–4793.

Shannon P, Markiel A, Ozier O, Baliga NS, Wang JT, Ramage D, Amin N, Schwikowski B, Ideker T. 2003. Cytoscape: a software environment for integrated models of biomolecular interaction networks. Genome Research **13**, 2498–2504.

Shi J, Wang Y, Wang C, *et al*. 2022. Linkage mapping combined with GWAS revealed the genetic structural relationship and candidate genes of maize flowering time-related traits. BMC Plant Biology **22**, 328.

Song J, Liu H, Zhuang H, Zhao C, Xu Y, Wu S, Qi J, Li J, Hettenhausen C, Wu J. 2017. Transcriptomics and alternative splicing analyses reveal large differences between maize lines B73 and Mo17 in response to aphid *Rhopalosiphum padi* infestation. Frontiers in Plant Science **8**, 1738.

Staswick PE, Tiryaki I. 2004. The oxylipin signal jasmonic acid is activated by an enzyme that conjugates it to isoleucine in Arabidopsis. The Plant Cell **16**, 2117–2127.

Stenzel I, Hause B, Maucher H, Pitzschke A, Miersch O, Ziegler J, Ryan CA, Wasternack C. 2003. Allene oxide cyclase dependence of the wound response and vascular bundle-specific generation of jasmonates in tomato--amplification in wound signalling. The Plant Journal **33**, 577–589.

Trapnell C, Roberts A, Goff L, Pertea G, Kim D, Kelley D, Pimentel H, Salzberg SL, Rinn JL, Pachter L. 2012. Differential gene and transcript expression analysis of RNA-seq experiments with TopHat and Cufflinks. Nature Protocols **7**, 562–578.

Tzin V, Fernandez-Pozo N, Richter A, *et al*. 2015a. Dynamic maize responses to aphid feeding are revealed by a time series of transcriptomic and metabolomic assays. Plant Physiology **169**, 1727–1743.

Tzin V, Lindsay PL, Christensen SA, Meihls LN, Blue LB, Jander G. 2015b. Genetic mapping shows intraspecific variation and transgressive

segregation for caterpillar-induced aphid resistance in maize. Molecular Ecology **24**, 5739–5750.

Wang B, Dong W, Li H, *et al*. 2022a. Molecular basis of (*E*)-β-farnesene-mediated aphid location in the predator *Eupeodes corollae*. Current Biology **32**, 951–962.e7.

Wang KLC, Hai L, Ecker JR. 2002. Ethylene biosynthesis and signaling networks. The Plant Cell **14**, S131–S151.

Wang Q, Liu X, Liu H, Fu Y, Cheng Y, Zhang L, Shi W, Zhang Y, Chen J. 2022b. Transcriptomic and metabolomic analysis of wheat kernels in response to the feeding of orange wheat blossom midges (*Sitodiplosis mosellana*) in the field. Journal of Agricultural and Food Chemistry **70**, 1477–1493.

Wang Y, Sun H, Wang H, Yang X, Xu Y, Yang Z, Xu C, Li P. 2021. Integrating transcriptome, co-expression and QTL-seq analysis reveals that primary root growth in maize is regulated via flavonoid biosynthesis and auxin signal transduction. Journal of Experimental Botany **72**, 4773–4795.

Wisecaver JH, Borowsky AT, Tzin V, Jander G, Kliebenstein DJ, Rokas A. 2017. A global coexpression network approach for connecting genes to specialized metabolic pathways in plants. The Plant Cell **29**, 944–959.

Wu J, Gao H, Zhu X, Li D. 2020. An ERF transcription factor enhances plant resistance to *Myzus persicae* and *Spodoptera litura*. Biotechnology & Biotechnological Equipment **34**, 946–954.

Wu X, Wang B, Xie F, Zhang L, Gong J, Zhu W, Li X, Feng F, Huang J. 2020. QTL mapping and transcriptome analysis identify candidate genes regulating pericarp thickness in sweet corn. BMC Plant Biology **20**, 117.

Yan J, Wang J, Li Q, Hwang JR, Patterson C, Zhang PH. 2003. AtCHIP, a U-box-containing E3 ubiquitin ligase, plays a critical role in temperature stress tolerance in Arabidopsis. Plant Physiology **132**, 861–869.

Yao L, Li Y, Ma C, Tong L, Du F, Xu M. 2020. Combined genome-wide association study and transcriptome analysis reveal candidate genes for resistance to *Fusarium* ear rot in maize. Journal of Integrative Plant Biology **62**, 1535–1551.

Yu G, Wang LG, Han Y, He QY. 2012. clusterProfiler: an R package for comparing biological themes among gene clusters. OMICS: A Journal of Integrative Biology **16**, 284–287.

Yu H, Wen D, Wang W, Geng L, Zhang Y, Xu J. 2015. Identification of genes putatively involved in chitin metabolism and insecticide detoxification in the rice leaf folder (*Cnaphalocrocis medinalis*) larvae through transcriptomic analysis. International Journal of Molecular Sciences **16**, 21873–21896.

Zeng W, Shi J, Qiu C, *et al*. 2020. Identification of a genomic region controlling thermotolerance at flowering in maize using a combination of whole genomic re-sequencing and bulked segregant analysis. Theoretical and Applied Genetics **133**, 2797–2810.

Zhang J, Li W, Lv P, *et al*. 2021. Whole-genome resequencing and transcriptome analysis provide insights on aphid-resistant quantitative trait loci/genes in *Sorghum bicolor*. Plant Breeding **140**, 618–629.

Zhao L, Zhao X, Francis F, Liu Y. 2021. Genome-wide identification and characterization of the *TPS* gene family in wheat (*Triticum aestivum* L.) and expression analysis in response to aphid damage. Acta Physiologiae Plantarum **43**, 64.

Zheng L, McMullen MD, Bauer E, Schön CC, Gierl A, Frey M. 2015. Prolonged expression of the BX1 signature enzyme is associated with a recombination hotspot in the benzoxazinoid gene cluster in *Zea mays*. Journal of Experimental Botany **66**, 3917–3930.

Zhou J, Zhang Y, Qi J, Chi Y, Fan B, Yu J, Chen Z. 2014. E3 ubiquitin ligase CHIP and NBR1-mediated selective autophagy protect additively against proteotoxicity in plant stress responses. PLoS Genetics **10**, e1004116.

Zogli P, Pingault L, Grover S, Louis J. 2020. Ento(o)mics: the intersection of 'omic' approaches to decipher plant defense against sap-sucking insect pests. Current Opinion in Plant Biology **56**, 153–161.